

Quasi-Maximum Likelihood Estimation for a Genuinely Unbalanced Dynamic Network Panel Data Model

Zhijian Wang^a, Xingbai Xu^{b,a,c,*}, and Tuo Liu^{a,b}

^aDepartment of Statistics and Data Science, School of Economics, Xiamen University

^bMOE Key Lab of Econometrics and Fujian Key Lab of Statistics, Wang Yanan Institute for Studies in Economics

^cPaula and Gregory Chow Institute for Studies in Economics, Xiamen University

January 1, 2026

Abstract

This paper develops a quasi-maximum likelihood estimator for genuinely unbalanced dynamic network panel data models with individual fixed effects. We propose a model that accommodates contemporaneous and lagged network spillovers, temporal dependence, and a listing effect that activates upon a unit's first appearance in the panel. We establish the consistency of the QMLE as both N and T go to infinity, derive its asymptotic distribution, and identify an asymptotic bias arising from incidental parameters when N is asymptotically large relative to T . Based on the asymptotic bias expression, we propose a bias-corrected estimator that is asymptotically unbiased and normally distributed under appropriate regularity conditions. Monte Carlo experiments examine the finite sample performance of the bias-corrected estimator across different criteria, including bias, RMSE, coverage probability, and the normality of the estimator. The empirical application to Airbnb listings from New Zealand and New York City reveals region-specific patterns in spatial and temporal price transmission, illustrating the importance of modeling genuine unbalancedness in dynamic network settings.

Keywords: Unbalanced Panel Data Model; Spatial Dynamic Panel Data Model; Dynamic Network Panel Data Model; Quasi-maximum Likelihood Estimation

Corresponding authors: Xingbai Xu and Tuo Liu. xuxingbai@xmu.edu.cn, liutuo2017@xmu.edu.cn.

1 Introduction

Panel data are widely used in economics and social science because they simultaneously capture individual heterogeneity and temporal dynamics. Compared with cross-sectional or time-series data, panel data provide richer information for analyzing both long-term relationships and short-term adjustments among variables. When units are spatially or network-connected—such as regions in an economic system, firms in a financial market, or individuals in a social platform—their outcomes often exhibit interdependence across both space and time. This has motivated the development of spatial dynamic panel data models, which integrate network interactions with temporal evolution. These models have been applied to a wide range of contexts, such as regional economics (Amidi et al. 2020), environmental systems (Chang et al. 2021), financial markets (Billé & Caporin 2022), and social networks (Han et al. 2021).

Unbalanced dynamic network panel data are commonly observed in real-world contexts such as regional rental markets, financial stock markets, and social networks. For instance, in stock markets, firms may enter or exit over time, as illustrated in Figure 1. The figure shows the historical retention status of CSI 300 and S&P 500 constituent stocks and indicates that a substantial share of constituents is replaced approximately every five years. Critically, these firms are interconnected through business partnerships or ownership ties, giving rise to a complex and evolving network structure. Together, the continuous turnover of units and the network links define an unbalanced dynamic network panel. Similarly, in social network studies, individuals exhibit heterogeneous temporal activity, and relationships evolve as users join or leave the network, which also constitutes a prototypical example of an unbalanced dynamic network panel.

Despite their empirical prevalence, theoretical work on dynamic spatial or network panels has overwhelmingly assumed balanced panels. Kapoor et al. (2007) study the estimation of static spatial panel data models. Yu et al. (2008) and Lee & Yu (2010) propose quasi-maximum likelihood estimation (QMLE) for spatial dynamic panel data models. Lee & Yu (2014) consider

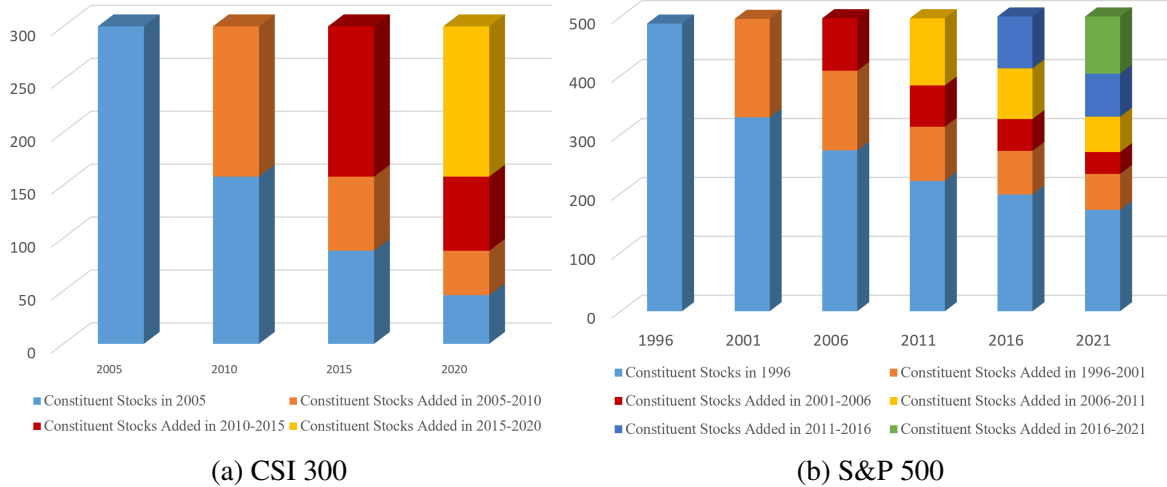


Figure 1: Historical retention status of CSI 300 and S&P 500 constituent stocks

the generalized method of moments (GMM) estimation for spatial dynamic panel data. [Lee & Yu \(2012\)](#) and [Qu et al. \(2017\)](#) extend the previous spatial dynamic panel data to scenarios with time-varying or endogenous spatial weight matrices. While these studies collectively enrich the methodological toolkit for spatial dynamic panel models, they all focus on balanced spatial panel data models.

In the field of unbalanced panel data, existing studies have focused on specific subtopics but lack integration with spatial dynamic structures. [Honoré \(1992\)](#), [Hu \(2002\)](#), and [Honoré & Hu \(2004\)](#) address censored unbalanced panel data models, while [Wooldridge \(1995\)](#) and [Kyriazidou \(1997\)](#) investigate unbalanced panels with sample selection bias. [Su et al. \(2025\)](#) develop estimation and inference methods for unbalanced panels with interactive fixed effects, and [Sasaki & Xin \(2017\)](#) study dynamic panel data with irregular time intervals. For spatial panel data, [Meng & Yang \(2025b\)](#) examine a static genuinely unbalanced spatial panel data model, while [Meng & Yang \(2025a\)](#) focus on static spatial panel data models with missing observations. None provide a unified framework for estimation and inference in unbalanced dynamic network panels.

This paper bridges this gap. We propose a quasi-maximum likelihood estimator (QMLE) for an unbalanced dynamic network panel model that captures network interactions and temporal

dynamics simultaneously, while explicitly accommodating unit entry and exit. We focus on panels that are *genuinely* unbalanced (Meng & Yang 2025b), **meaning that the unbalancedness is driven by the entry and exit of units rather than by missing observations**. This specification allows us to avoid modeling any data missing process. Our main contributions and results are as follows.

1. We propose model (1) to characterize genuinely unbalanced dynamic network panels. We introduce a common listing effect, which replaces lagged terms with a listing effect in a unit's first active period. This listing effect reflects a unified average entry shock. Building on this model, we develop the QMLE estimation and statistical inference procedures.
2. Since the size and the elements of the network weight matrices vary over time, our setup is different from that of balanced spatial panel data models. As a result, we need to establish a number of new results for linear–quadratic forms, which extend the linear–quadratic theory from balanced spatial dynamic panel data models to unbalanced ones. We believe that these new results are also applicable to future studies of unbalanced network panel data models.
3. We establish the consistency of the QMLE as both N and T go to infinity, and further derive its asymptotic distribution. Due to incidental parameters, the QMLE exhibits an $O(\frac{1}{T})$ asymptotic bias and a noncentered normal limiting distribution, when N grows proportionally to T . Based on the asymptotic analysis, we derive a bias-corrected estimator that is asymptotically unbiased and normally distributed as long as $\frac{N}{T^3} \rightarrow 0$.

We examine the finite sample performance of the estimator through Monte Carlo simulations. Furthermore, we apply our model to study an empirical Airbnb listing dataset. We compare the estimated results across different regions and spatial scales to analyze the similarities and differences in the dynamic pricing behavior of Airbnb listings across cities.

This paper is organized as follows. In Section 2, we introduce our model and derive the concentrated log-likelihood function. Section 3 establishes the consistency and asymptotic distribution of

the QMLE. In addition, based on the asymptotic bias of the QMLE, we derive a bias-corrected estimator. Section 4 uses Monte Carlo simulations to examine the consistency and asymptotic normality of both the original QMLE and its bias-corrected counterpart. Section 5 presents an empirical evaluation of the model’s performance using real-world data. Section 6 concludes the paper. All proofs are collected in the appendices.

Notation

We define ι_N as the N -dimensional column vector of ones, and I_N as the N -dimensional identity matrix. For any matrix B , B_{ij} represents the (i, j) -th element of the matrix B . $B_{i \cdot}$ and $B_{\cdot j}$ are the i -th row and j -th column of B , respectively. Denote $\|B\|_1 \equiv \sup_{1 \leq j \leq N} \sum_{i=1}^N |B_{ij}|$ and $\|B\|_\infty \equiv \sup_{1 \leq i \leq N} \sum_{j=1}^N |B_{ij}|$ as the one-norm and the infinity-norm for matrix B , respectively. For a vector C , denote $\|C\|_1 = \sum_{i=1}^N |C_i|$, $\|C\|_\infty = \sup_i |C_i|$ and $\|C\|_2 \equiv (\sum_{i=1}^N C_i^2)^{\frac{1}{2}}$ as the Euclidean norm of vector C . Let $\text{tr}(B)$ denote the trace of matrix B and $|B|$ denote the determinant of B . Define $\sup_t B_t$ as the element-wise supremum of the matrix sequence $\{B_t\}$, which means that $(\sup_t B_t)_{ij} = \sup_t B_{t,ij}$ for $i, j = 1, \dots, N$. Also, $\text{abs}(B)$ represents the element-wise absolute value of the matrix B , i.e., $[\text{abs}(B)]_{ij} = |B_{ij}|$. For any square matrix B , B^- denotes the strictly lower triangular part of B , obtained by setting the diagonal and upper triangular entries to zero. The notation $\text{diag}(b_1, \dots, b_N)$ represents a diagonal matrix with diagonal entries b_1, b_2, \dots, b_N . Moreover, $\text{blkdiag}(B_1, \dots, B_T)$ forms a block-diagonal matrix by the given submatrices. For brevity, the transposes of symmetrically positioned submatrices in a symmetric matrix are sometimes denoted by $*$. Var and Cov represent the variance and covariance of random variables, respectively.

2 The Model and Concentrated Likelihood Function

2.1 The Model

Consider a genuinely unbalanced dynamic network panel, where nodes are fully observed during each period (i.e., there are no missing data), and nodes that are not listed do not have any impact on the whole network. Suppose that we have observations for a network of N nodes over T time periods. However, for the i -th node, we only have a total of T_i consecutive observations¹. In the t -th time period, observed nodes may drop out of the network, and new nodes may join the network. We can only observe N_t nodes in period t and let $\mathbb{I}_t = \{i_1, i_2, \dots, i_{N_t}\}$ denote the set of indices of nodes observed. Their corresponding attributes are (y_{it}, x'_{it}) for each $i \in \mathbb{I}_t$, where y_{it} is a scalar dependent variable and x_{it} is a k -dimensional vector of regressors. The sample size of data available is $n = \sum_{t=1}^T N_t$.

Then we can establish the following model: for $t = 1, 2, \dots, T$ and $i \in \mathbb{I}_t$,

$$y_{it} = \rho_0 \sum_{j \in \mathbb{I}_t} w_{ij,t} y_{jt} + d_{i,t-1} (\lambda_0 \sum_{j \in \mathbb{I}_{t-1}} m_{ij,t} y_{j,t-1} + \nu_0 y_{i,t-1}) + d_{it} (1 - d_{i,t-1}) \gamma_0 + x'_{it} \beta_0 + \alpha_{i0} + v_{it}, \quad (1)$$

where $w_{ij,t}$ and $m_{ij,t}$ are predefined network weights, and d_{it} is an indicator that equals 1 if y_{it} is observed and 0 otherwise. γ_0 and α_{i0} are unknown listing and individual fixed effects, respectively, where the listing effect only takes effect at the first appearance of each individual, and the effect is identical for each individual. The above model assumes that y_{it} is not only affected by its own covariates and the current network structure, but also by the fixed listing effect if node i has just been listed or by its own lagged outcome and the lagged network state if node i was already present. Since we only model the nodes that appear at $t = 0$ or later and cannot observe the data for $t < 0$, to simplify the analysis, we ignore the impact of nodes that existed only before $t = 0$.

¹We assume that each individual enters the market only once. It is not hard to generalize this condition to allow for entering and leaving for multiple times for this same individual.

Denote $Y_t = (y_{i_1 t}, \dots, y_{i_{N_t} t})'$ as an N_t -dimensional column vector, $X_t = (x_{i_1 t}, \dots, x_{i_{N_t} t})'$ as an $N_t \times k$ matrix, and $V_t = (v_{i_1 t}, \dots, v_{i_{N_t} t})'$ as an N_t -dimensional column vector, where $i_1, \dots, i_{N_t} \in \mathbb{I}_t$. Define $\alpha_0 = (\alpha_{10}, \alpha_{20}, \dots, \alpha_{N0})'$. The $N_t \times N$ matrix D_t is obtained by removing the rows corresponding to unobserved nodes during period t from I_N . Then the above model can be written in the following matrix form: for $t = 1, 2, \dots, T$,

$$Y_t = \rho_0 W_t Y_t + \lambda_0 D_t (I_N - F_t) D_t' M_t Y_{t-1} + \nu_0 D_t D_{t-1}' Y_{t-1} + \gamma_0 D_t F_t \iota_N + X_t \beta_0 + D_t \alpha_0 + V_t. \quad (2)$$

In the above model, W_t and M_t are $N_t \times N_t$ and $N_t \times N_{t-1}$ network weight matrices, respectively. The elements of W_t and M_t are defined as:

$$(W_t)_{k,l} \equiv w_{i_k i_l, t}, \quad \text{for } k, l = 1, 2, \dots, N_t \text{ and } i_k, i_l \in \mathbb{I}_t,$$

$$(M_t)_{k,l} \equiv m_{i_k j_l, t}, \quad \text{for } k = 1, 2, \dots, N_t, l = 1, 2, \dots, N_{t-1}, i_k \in \mathbb{I}_t \text{ and } j_l \in \mathbb{I}_{t-1}.$$

The N -dimensional diagonal matrix $F_t \equiv D_t' D_t (I_N - D_{t-1}' D_{t-1}) = \text{diag}(d_{1t}(1 - d_{1,t-1}), \dots, d_{N,t}(1 - d_{N,t-1}))$ is the listing index matrix. $F_t \iota_N$ is sparser than other covariates because, over all T periods, fewer than N individuals can newly join the network. According to equation (2),

$$\begin{aligned} Y_t &= S_t^{-1} [\lambda_0 D_t (I_N - F_t) D_t' M_t Y_{t-1} + \nu_0 D_t D_{t-1}' Y_{t-1} + \gamma_0 D_t F_t \iota_N + X_t \beta_0 + D_t \alpha_0 + V_t] \\ &= S_t^{-1} D_t [\lambda_0 (I_N - F_t) D_t' M_t + \nu_0 D_{t-1}'] Y_{t-1} + S_t^{-1} [D_t (\gamma_0 F_t \iota_N + \alpha_0) + X_t \beta_0 + V_t] \end{aligned}$$

where $S_t \equiv I_{N_t} - \rho_0 W_t$ is assumed to be invertible. Denote $A_t \equiv D_t [\lambda_0 (I_N - F_t) D_t' M_t + \nu_0 D_{t-1}'] S_t^{-1}$. Assuming that the following infinite summation is well-defined, we obtain by

continuous substitution that

$$Y_t = \sum_{h=0}^{\infty} S_t^{-1} A_t^{(h)} [D_{t-h}(\gamma_0 F_{t-h} \iota_N + \alpha_0) + X_{t-h} \beta_0 + V_{t-h}] \equiv \mathcal{E}_t + \mathcal{X}_t \beta_0 + \mathcal{V}_t, \quad (3)$$

where $A_t^{(h)} \equiv A_t A_{t-1} \cdots A_{t-h+1}$ for $h = 1, 2, \dots$ and $A_t^{(0)} \equiv I_{N_t}$, $\mathcal{E}_t \equiv \sum_{h=0}^{\infty} S_t^{-1} A_t^{(h)} D_{t-h}(\gamma_0 F_{t-h} \iota_N + \alpha_0)$, $\mathcal{X}_t \equiv \sum_{h=0}^{\infty} S_t^{-1} A_t^{(h)} X_{t-h}$ and $\mathcal{V}_t \equiv \sum_{h=0}^{\infty} S_t^{-1} A_t^{(h)} V_{t-h}$. From the above decomposition, Y_t can be viewed as an infinite moving average representation. We establish the law of large numbers and the central limit theorem based on this decomposition in the lemmas in Supplementary Appendix A.

2.2 Quasi-Maximum Likelihood Method

Define $Z_t \equiv (D_t(I_N - F_t)D_t' M_t Y_{t-1}, D_t D_{t-1}' Y_{t-1}, D_t F_t \iota_N, X_t)$, $\delta_0 \equiv (\lambda_0, \nu_0, \gamma_0, \beta_0')'$. Then model (2) can be simplified to

$$Y_t = \rho_0 W_t Y_t + Z_t \delta_0 + D_t \alpha_0 + V_t. \quad (4)$$

Stacking the matrices and vectors in model (4) for $t = 1, 2, \dots, T$, we have

$$\mathbb{Y} = \rho_0 \mathbb{W} \mathbb{Y} + \mathbb{Z} \delta_0 + \mathbb{D} \alpha_0 + \mathbb{V}, \quad (5)$$

where $\mathbb{Y} = (Y_1', \dots, Y_T')'$, $\mathbb{W} = \text{blkdiag}(W_1, \dots, W_T)$, $\mathbb{Z} = (Z_1', \dots, Z_T')'$, $\mathbb{D} = (D_1', \dots, D_T')'$ and $\mathbb{V} = (V_1', \dots, V_T')'$. Note that $\mathbb{D}' \mathbb{D} = \sum_{t=1}^T D_t' D_t = \sum_{t=1}^T \text{diag}(d_{1t}, d_{2t}, \dots, d_{Nt}) = \text{diag}(T_1, T_2, \dots, T_N) \equiv \mathcal{T}$. Assume v_{it} 's are i.i.d. random variables with mean 0 and variance σ_0^2 . Denote the parameters of interest as $\theta = (\rho, \delta', \sigma^2)'$ and let $\zeta = (\rho, \delta')$. Then the

log-likelihood function of model (5) is

$$L_n(\theta, \alpha) = -\frac{n}{2} \ln 2\pi - \frac{n}{2} \ln \sigma^2 + \ln |\mathbb{S}(\rho)| - \frac{1}{2\sigma^2} \mathbb{V}'(\zeta, \alpha) \mathbb{V}(\zeta, \alpha), \quad (6)$$

where $\mathbb{S}(\rho) \equiv I_n - \rho \mathbb{W}$ and $\mathbb{V}(\zeta, \alpha) \equiv \mathbb{S}(\rho) \mathbb{Y} - \mathbb{Z} \delta - \mathbb{D} \alpha$. Given ζ , $L_n(\theta, \alpha)$ is maximized at

$$\hat{\alpha}(\zeta) = (\mathbb{D}' \mathbb{D})^{-1} \mathbb{D}' (\mathbb{S}(\rho) \mathbb{Y} - \mathbb{Z} \delta).$$

Substituting $\hat{\alpha}$ into (6), we obtain our estimator $\hat{\theta}$ by maximizing the following concentrated log-likelihood function

$$L_n^c(\theta) = -\frac{n}{2} \ln 2\pi - \frac{n}{2} \ln \sigma^2 + \ln |\mathbb{S}(\rho)| - \frac{1}{2\sigma^2} \tilde{\mathbb{V}}'(\zeta) \tilde{\mathbb{V}}(\zeta), \quad (7)$$

where $\tilde{\mathbb{V}}(\zeta) \equiv \mathbb{S}(\rho) \mathbb{Y} - \mathbb{Z} \delta - \mathbb{D} \hat{\alpha} = \mathbb{Q}(\mathbb{S}(\rho) \mathbb{Y} - \mathbb{Z} \delta)$ and $\mathbb{Q} \equiv I_n - \mathbb{P}$, $\mathbb{P} \equiv \mathbb{D}(\mathbb{D}' \mathbb{D})^{-1} \mathbb{D}'$.

Moreover, the corresponding expected value function of $L_n^c(\theta)$ is

$$Q_n(\theta) \equiv E[L_n^c(\theta)] = -\frac{n}{2} \ln 2\pi - \frac{n}{2} \ln \sigma^2 + \ln |\mathbb{S}(\rho)| - \frac{1}{2\sigma^2} E[\tilde{\mathbb{V}}'(\zeta) \tilde{\mathbb{V}}(\zeta)]. \quad (8)$$

We derive the asymptotic properties of the estimators based on $L_n^c(\theta)$ and $Q_n(\theta)$. In practice, we further concentrate out δ and σ^2 to accelerate computation, that is, we optimize

$$L_n^{cc}(\rho) \equiv -\frac{n}{2} \ln 2\pi - \frac{n}{2} \ln \hat{\sigma}^2 + \ln |\mathbb{S}(\rho)| - \frac{n}{2}$$

instead, where $\hat{\sigma}^2 = \frac{1}{n} (\mathbb{S}(\rho) \mathbb{Y} - \mathbb{Z} \hat{\delta})' \mathbb{Q} (\mathbb{S}(\rho) \mathbb{Y} - \mathbb{Z} \hat{\delta}) = \frac{1}{n} \mathbb{Y}' \mathbb{S}(\rho)' [I_n - \mathbb{Q} \mathbb{Z} (\mathbb{Z}' \mathbb{Q} \mathbb{Z})^{-1} \mathbb{Z}' \mathbb{Q}] \mathbb{S}(\rho) \mathbb{Y}$.

3 Asymptotic properties of QMLE

3.1 Consistency of QMLE

In the proof of consistency, we first establish the consistency of all parameters except γ , and then prove the consistency of γ . Define $\mathbb{Z}^{(-\gamma)}$ as the matrix obtained by removing the third column from \mathbb{Z} , and let $\mathbb{Z}^{(\gamma)}$ be the third column of \mathbb{Z} . To establish the consistency of QMLE, the following assumptions are needed.

Assumption 1 *The unbalancedness of the model is nonstochastic, which means that d_{it} and D_t are nonstochastic for all i and t . There is a lower bound on the number of observations for all individuals, i.e., $T_i \geq c_T T$ for all i , where $c_T > 0$ is a constant that does not vary with N or T . Additionally, $N_0 < c_N N$, where N_0 denotes the number of units observed at $t = 0$ and $0 < c_N < 1$ is a constant that does not vary with N or T .*

Assumption 2 *The error terms v_{it} 's are i.i.d. across i and t with mean 0, variance σ_0^2 , third order moment μ_3 and fourth order moment μ_4 . $E|v_{it}|^{4+2\eta} < \infty$ for some $\eta > 0$.*

Assumption 3 $\sup_{\rho \in \Lambda} \sup_{N,T} \sup_t \|\rho W_t\|_\infty < 1$, where Λ is the parameter space of ρ . Moreover, Λ is compact and ρ_0 lies in the interior of Λ .

Assumption 4 *The elements of x_{it} and α_{i0} are nonstochastic and bounded uniformly in i , t , N and T . $\mathbb{Z}'\mathbb{Q}\mathbb{Z}$ is nonsingular. Also, $\lim_{n \rightarrow \infty} \frac{1}{n} E(\mathbb{Z}^{(-\gamma)'} \mathbb{Q} \mathbb{Z}^{(-\gamma)})$ exists and is nonsingular, where $n = \sum_{t=1}^T N_t$ is the total sample size.*

Assumption 5 *The sequences of matrices $\{W_t\}$, $\{M_t\}$ and $\{S_t^{-1}\}$ are nonstochastic and uniformly bounded in row and column sum norms (for short, UB)² uniformly for t . Moreover,*

$$\max\left(\left\|\sup_t \text{abs}(D_t' S_t^{-1} D_t)\right\|_\infty, \left\|\sup_t \text{abs}(D_t' W_t D_t)\right\|_\infty, \left\|\sup_t \text{abs}(D_t' M_t D_{t-1})\right\|_\infty\right) < \infty.$$

²We say a $N \times N$ matrix B is UB if $\sup_N \max\{\|B\|_1, \|B\|_\infty\} < \infty$. We say a sequence of $N_t \times N_t$ matrices $\{B_t\}$ is UB uniformly for t if $\sup_{N,T} \sup_t \max\{\|B_t\|_1, \|B_t\|_\infty\} < \infty$.

Assumption 6 $\sum_{h=1}^{\infty} \text{abs} \left(D_t' A_t^{(h)} D_{t-h} \right)$ and $\sum_{h=t}^{\infty} \text{abs} \left(D_h' A_h^{(h-t)} D_t \right)$ are UB uniformly for t .

Assumption 7 N is a nondecreasing function of T , and N will go to infinity as T goes to infinity.

Assumption 1 regulates the unbalancedness of the panel, where we assume the unbalancedness to be nonstochastic. We will leave the more complicated case where d_{it} is stochastic for future research. A lower bound on T_i is imposed to ensure the consistency of the estimator for α , and an upper bound on N_0 is imposed to guarantee the consistency of the estimator for γ , as it requires sufficiently many observed listing effects. If this condition is not satisfied, a similar asymptotic analysis can still be conducted, but the convergence rate of $\hat{\gamma}$ will change. Assumption 2 provides regularity assumptions for v_{it} . Similar assumptions are adopted in [Lee \(2004\)](#) and [Yu et al. \(2008\)](#). Assumption 3 is a standard assumption for spatial (or network) panel data models. It implies that $S_t(\rho)^{-1}$ exists and

$$\sup_{\rho \in \Lambda} \sup_{N,T} \sup_t \|S_t(\rho)^{-1}\|_{\infty} < \infty, \quad (9)$$

which is proved in equation (S.28) in the supplementary materials of [Wu et al. \(2025\)](#). Although the assumption that ρ_0 lies in the interior of the parameter space is in fact imposed for simplicity and not required consistency, we state the conditions jointly for notational convenience. Assumption 4 rules out multicollinearity, ensuring that δ is estimable. We consider fixed design in this paper as in [Lee \(2004, 2007\)](#), [Yu et al. \(2008\)](#) and [Lee & Yu \(2014\)](#), among others. This assumption can be relaxed to allow for stochastic exogenous variables by using the near-epoch dependence theory in [Jenish & Prucha \(2012\)](#) or the functional dependence theory in [Wu et al. \(2025\)](#). The proof is similar to the proof under fixed design. Assumption 5 is a standard condition in the literature of spatial and network econometrics. See [Lee \(2004, 2007\)](#), [Yu et al. \(2008\)](#) and [Lee & Yu \(2014\)](#). The assumption that $\sup_{N,T} \sup_t \|S_t^{-1}\|_{\infty} < \infty$ can in fact be ensured by equation (9). Moreover, Assumption 5 implies that $\{S_t(\rho)^{-1}\}$ is UB uniformly in a neighborhood of ρ_0 , from Lemma A.3 of [Lee \(2004\)](#). Assumption 6 restricts the joint effect of network spillovers and temporal

dynamics, which is a common assumption in dynamic network panel data, such as Assumption 6 in [Yu et al. \(2008\)](#), Assumption 7 in [Lee & Yu \(2014\)](#) and Assumption 6 in [Lee & Yu \(2012\)](#). Assumptions 5 and 6 are imposed to establish a law of large numbers and a central limit theorem for certain quadratic forms of the network lag spillover term $M_t Y_{t-1}$ and the temporal lag term Y_{t-1} . Assumption 7 means that we consider a large- N and large- T setting, in which the QMLE is consistent. For short dynamic network panel data models other estimation methods, (e.g., GMM) are required.

Denote $\mathbb{S}_0 \equiv \mathbb{S}(\rho_0)$, $\mathbb{G}(\rho) \equiv \mathbb{W}\mathbb{S}(\rho)^{-1}$ and $\mathbb{G}_0 \equiv \mathbb{W}\mathbb{S}_0^{-1}$. Define $\mathcal{H}^{(-\gamma)} \equiv \frac{1}{n}(\mathbb{G}_0 \mathbb{Z} \delta_0 + \mathbb{G}_0 \mathbb{D} \alpha_0, \mathbb{Z}^{(-\gamma)})' \mathbb{Q}(\mathbb{G}_0 \mathbb{Z} \delta_0 + \mathbb{G}_0 \mathbb{D} \alpha_0, \mathbb{Z}^{(-\gamma)})$ and $\sigma_n^2 \equiv \frac{\sigma_0^2}{n} \text{tr}[(\mathbb{S}(\rho) \mathbb{S}_0^{-1})' \mathbb{S}(\rho) \mathbb{S}_0^{-1}]$. As in [Yu et al. \(2008\)](#), the following assumption is needed to establish the global identification condition required for consistency.

Assumption 8 *At least one of the following two conditions is satisfied: (i) $\lim_{n \rightarrow \infty} E\mathcal{H}^{(-\gamma)}$ exists and is nonsingular. (ii) $\lim_{n \rightarrow \infty} \left(\frac{1}{n} \ln |\sigma_0^2 \mathbb{S}_0^{-1} \mathbb{S}_0^{-1}| - \frac{1}{n} \ln |\sigma_n^2 \mathbb{S}(\rho)^{-1} \mathbb{S}(\rho)^{-1}| \right) \neq 0$ for $\rho \neq \rho_0$.*

Theorem 1 *Under Assumptions 1-8, $\hat{\theta} \xrightarrow{p} \theta_0$.*

3.2 Asymptotic Distribution of QMLE

Since we have concentrated out the N individual fixed effects from the log likelihood function, the QMLE is subject to the incidental parameters problem, which induces an asymptotic bias in the estimator ([Meng & Yang 2025b](#)). We derive the asymptotic distribution of $\hat{\theta}$ by performing a Taylor expansion of $\frac{\partial L_n^c(\hat{\theta})}{\partial \theta}$ around θ_0 . The first and second order derivatives of $L_n^c(\theta)$ are derived in Supplementary Appendix B. According to (3), denote $Z_t^\circ \equiv (D_t(I_N - F_t)D_t' M_t \mathcal{V}_{t-1}, D_t D_{t-1}' \mathcal{V}_{t-1}, \mathbf{0}_{N_t \times (k+1)})$ and $\mathbb{Z}^\circ \equiv (Z_1^\circ, \dots, Z_T^\circ)'$. We decompose $\mathbb{Q}\mathbb{Z}$ into $\mathbb{Q}\mathbb{Z} = \tilde{\mathbb{Z}}^* - \tilde{\mathbb{Z}}^\circ$, where $\tilde{\mathbb{Z}}^\circ \equiv \mathbb{P}\mathbb{Z}^\circ$ and $\tilde{\mathbb{Z}}^* = \mathbb{Q}\mathbb{Z} + \tilde{\mathbb{Z}}^\circ$. Note that Z_t° is independent of V_s when $t \leq s$, and $\tilde{\mathbb{Z}}^* = \mathbb{Q}\mathbb{Z} + \tilde{\mathbb{Z}}^\circ = \mathbb{Q}(\mathbb{Z} - \mathbb{Z}^\circ) + \mathbb{Z}^\circ$, where $\mathbb{Z} - \mathbb{Z}^\circ$ is nonstochastic. Decompose $\tilde{\mathbb{Z}}^*$ into N_t -dimensional vectors $\tilde{Z}_1^*, \dots, \tilde{Z}_T^*$ such that $\tilde{\mathbb{Z}}^* = (\tilde{Z}_1^*, \dots, \tilde{Z}_T^*)'$. Therefore,

\tilde{Z}_t^* is independent of V_s when $t \leq s$. But $\tilde{\mathbb{Z}}^\circ$ is correlated with \mathbb{V} , as proved in Lemma 11 in Supplementary Appendix A.

Similarly, we can decompose $\mathbb{Q}\mathbb{G}_0\mathbb{Z} = \widetilde{\mathbb{G}_0\mathbb{Z}}^* - \widetilde{\mathbb{G}_0\mathbb{Z}}^\circ$, where $\widetilde{\mathbb{G}_0\mathbb{Z}}^\circ \equiv \mathbb{P}\mathbb{G}_0\mathbb{Z}^\circ$ and $\widetilde{\mathbb{G}_0\mathbb{Z}}^* = \mathbb{Q}\mathbb{G}_0\mathbb{Z} + \widetilde{\mathbb{G}_0\mathbb{Z}}^\circ$. Further, decompose $\widetilde{\mathbb{G}_0\mathbb{Z}}^*$ into N_t -dimensional vectors $\widetilde{GZ}_1^*, \dots, \widetilde{GZ}_T^*$ such that $\widetilde{\mathbb{G}_0\mathbb{Z}}^* = (\widetilde{GZ}_1^{*\prime}, \dots, \widetilde{GZ}_T^{*\prime})'$. Similarly, \widetilde{GZ}_t^* is independent of V_s when $t \leq s$, whereas $\widetilde{\mathbb{G}_0\mathbb{Z}}^\circ$ is correlated with \mathbb{V} .

Denote $\Gamma = \text{blkdiag}(I_3, \sqrt{T}, I_{k+1})$ and $\tilde{\Gamma} = \text{blkdiag}(I_2, \sqrt{T}, I_k)$, then we can rewrite $\frac{1}{\sqrt{n}}\Gamma \frac{\partial L_n^c(\theta_0)}{\partial \theta} = \frac{1}{\sqrt{n}}\Gamma \frac{\partial L_n^{c*}(\theta_0)}{\partial \theta} - \Delta_n$, where

$$\frac{1}{\sqrt{n}}\Gamma \frac{\partial L_n^{c*}(\theta_0)}{\partial \theta} = \begin{pmatrix} \frac{1}{\sqrt{n}\sigma_0^2}(\mathbb{G}_0\mathbb{D}\alpha_0)'Q\mathbb{V} + \frac{1}{\sqrt{n}\sigma_0^2}\mathbb{V}'\mathbb{G}_0\mathbb{V} + \frac{1}{\sqrt{n}\sigma_0^2}(\widetilde{\mathbb{G}_0\mathbb{Z}}^* \delta_0)' \mathbb{V} - \frac{1}{\sqrt{n}}\text{tr}(\mathbb{G}_0) \\ \frac{1}{\sqrt{n}\sigma_0^2}\tilde{\Gamma}\widetilde{\mathbb{Z}}^{*\prime}\mathbb{V} \\ -\frac{n}{2\sqrt{n}\sigma_0^2} + \frac{1}{2\sqrt{n}\sigma_0^4}\mathbb{V}'\mathbb{V} \end{pmatrix},$$

and

$$\Delta_n = \begin{pmatrix} \frac{1}{\sqrt{n}\sigma_0^2}\mathbb{V}'\mathbb{G}_0'\mathbb{P}\mathbb{V} + \frac{1}{\sqrt{n}\sigma_0^2}(\widetilde{\mathbb{G}_0\mathbb{Z}}^\circ \delta_0)' \mathbb{V} \\ \frac{1}{\sqrt{n}\sigma_0^2}\tilde{\Gamma}\widetilde{\mathbb{Z}}^{\circ\prime}\mathbb{V} \\ \frac{1}{2\sqrt{n}\sigma_0^4}\mathbb{V}'\mathbb{P}\mathbb{V} \end{pmatrix}.$$

This decomposes $\frac{\partial L_n^c(\theta_0)}{\partial \theta}$ into two components: a mean zero term $\frac{\partial L_n^{c*}(\theta_0)}{\partial \theta}$ and a nonzero mean term Δ_n . Δ_n can be regarded as the source of asymptotic bias arising from the estimation of fixed effects. As derived in Supplementary Appendix B.2,

$$E \left(\frac{1}{\sqrt{n}}\Gamma \frac{\partial L_n^{c*}(\theta_0)}{\partial \theta} \cdot \frac{1}{\sqrt{n}} \frac{\partial L_n^{c*}(\theta_0)}{\partial \theta'} \Gamma \right) = \Gamma \Sigma_{\theta_0, n} \Gamma + \Gamma \Omega_{\theta_0, n} \Gamma + O\left(\frac{1}{T}\right).$$

Denote $\Sigma_{\theta_0} \equiv \lim_{n \rightarrow \infty} \Gamma \Sigma_{\theta_0, n} \Gamma$, $\Omega_{\theta_0} \equiv \lim_{n \rightarrow \infty} \Gamma \Omega_{\theta_0, n} \Gamma$, then

$$\lim_{n \rightarrow \infty} E \left(\frac{1}{\sqrt{n}} \Gamma \frac{\partial L_n^{c*}(\theta_0)}{\partial \theta} \cdot \frac{1}{\sqrt{n}} \frac{\partial L_n^{c*}(\theta_0)}{\partial \theta'} \Gamma \right) = \Sigma_{\theta_0} + \Omega_{\theta_0}. \quad (10)$$

The asymptotic distribution of $\frac{\partial L_n^{c*}(\theta_0)}{\partial \theta}$ can be derived by applying the central limit theorem for martingale difference sequences, as proved in Lemma 18 in Supplementary Appendix A. Furthermore, as derived in Supplementary Appendix B.4, we have $\Delta_n = \sqrt{\frac{N}{c_u T}} \varphi_n(\theta_0) + O_p\left(\frac{1}{\sqrt{T}}\right)$, where $c_u \equiv \frac{n}{NT}$, $\varphi_n(\theta_0) = O(1)$ and $\varphi_n(\theta)$ is defined in equation (B.6) in Supplementary Appendix B.4.

The following assumption ensures the nonsingularity of the information matrix Σ_{θ_0} .

Assumption 9 At least one of the following two conditions is satisfied: (i) $\lim_{n \rightarrow \infty} E \mathcal{H}^{(-\gamma)}$ exists and is nonsingular. (ii) $\lim_{n \rightarrow \infty} \frac{1}{n} \left(\text{tr}(\mathbb{G}_0^2 + \mathbb{G}_0' \mathbb{G}_0) - \frac{2}{n} [\text{tr}(\mathbb{G}_0)]^2 \right) \neq 0$.

Theorem 2 Under Assumptions 1-9,

$$\sqrt{n} \Gamma^{-1} \left[\hat{\theta} - \left(\theta_0 - \frac{\Sigma_{\theta_0, n}^{-1} \varphi_n(\theta_0)}{c_u T} \right) \right] + O_p \left(\max \left\{ \frac{1}{\sqrt{T}}, \sqrt{\frac{N}{T^3}} \right\} \right) \xrightarrow{d} N \left(0, \Sigma_{\theta_0}^{-1} (\Sigma_{\theta_0} + \Omega_{\theta_0}) \Sigma_{\theta_0}^{-1} \right), \quad (11)$$

where $\Sigma_{\theta_0, n}^{-1} \varphi_n(\theta_0)$ is $O(1)$.

If error terms v_{it} 's are normal, $\Omega_{\theta_0} = 0$ and the asymptotic variance of equation (11) becomes $\Sigma_{\theta_0}^{-1}$.

Theorem 2 shows that $\hat{\theta}$ exhibits an asymptotic bias $-\Sigma_{\theta_0, n}^{-1} \varphi_n(\theta_0)/(c_u T)$. It also shows that $\hat{\theta}^{(-\gamma)}$ is \sqrt{n} -consistent and $\hat{\gamma}$ is $\sqrt{c_u N}$ -consistent. When $N/T \rightarrow 0$, $\hat{\theta}$ is consistent and asymptotically centered normal, which means

$$\sqrt{n} \Gamma^{-1} (\hat{\theta} - \theta_0) \xrightarrow{d} N \left(0, \Sigma_{\theta_0}^{-1} (\Sigma_{\theta_0} + \Omega_{\theta_0}) \Sigma_{\theta_0}^{-1} \right).$$

3.3 Bias Correction

According to (11), $\hat{\theta}$ exhibits the bias $-\Sigma_{\theta_0, n}^{-1} \varphi_n(\theta_0) / (c_u T)$, thus a bias-corrected counterpart of $\hat{\theta}$ takes the form

$$\hat{\theta}^1 = \hat{\theta} + \frac{\hat{B}_n}{c_u T},$$

where $\hat{B}_n = \left[\left(-\frac{1}{n} \frac{\partial^2 L_n^c(\theta)}{\partial \theta \partial \theta'} \right)^{-1} \varphi_n(\theta) \right]_{\theta=\hat{\theta}}$.

Assumption 10 $\sum_{h=0}^{T-t} D_t A_t^{(h)}(\theta) D_{t-h}$ and $\frac{\partial}{\partial \theta} \sum_{h=0}^{T-t} D_t A_t^{(h)}(\theta) D_{t-h}$ are UB uniformly in a neighborhood of θ_0 over t .

Theorem 3 Under Assumptions 1-10, if $N/T^3 \rightarrow 0$,

$$\sqrt{n} \Gamma^{-1} (\hat{\theta}^1 - \theta_0) \xrightarrow{d} N \left(0, \Sigma_{\theta_0}^{-1} (\Sigma_{\theta_0} + \Omega_{\theta_0}) \Sigma_{\theta_0}^{-1} \right).$$

Hence, the estimator after bias correction is asymptotically normal and centered around θ_0 as long as T grows faster than $N^{\frac{1}{3}}$.

4 Monte Carlo Simulation

4.1 Data-Generating Process

In the simulation study, we generate an unbalanced panel dataset of size $N \times (T + 21)$, where the first 20 periods are used only to generate a stable Y_0 and the remaining $T + 1$ periods are used for estimation (set $t = 0$ at the 21st period). In order to simulate unbalancedness in the panel, we randomly assign to each node a contiguous observation window within the $T + 1$ periods. Specifically, we first draw the observation duration for each observed node: $T_i \sim \text{GE}(\frac{p}{T}) + 2$, where GE denotes the geometric distribution supported on nonnegative integers and p is the parameter of the geometric distribution. Based on the T_i we generated, if $T_i \geq T + 1$, then node i

is observed for $T + 1$ periods. Otherwise, we place the contiguous observation window of length T_i uniformly at random within the $(T + 1)$ -period horizon. By tuning the parameter p , we can control the unbalancedness proportion of the panel, which is defined as $UP \equiv 1 - \frac{n}{NT}$, around a target mean level.

We generate X_t, α_0 independently from the standard normal distribution. We simulate the dependent variable using a 20-period pre-sample burn-in. For individuals already observed in period 0, we initialize their outcome at $t = -20$ as $y_{i,-20} \sim N(0, 1)$, drawn independently across units. The subsequent observations ($t = -19, \dots, 0$) are then generated iteratively according to equation (2). Given Y_0 , we can generate Y_1, \dots, Y_T iteratively according to equation (2). For the network weight matrix, we first construct an $N \times N$ adjacency matrix A by rook contiguity, and then row-normalize $D_t A D_t'$ and $D_t A D_{t-1}'$, respectively to obtain the weight matrices W_t and M_t .

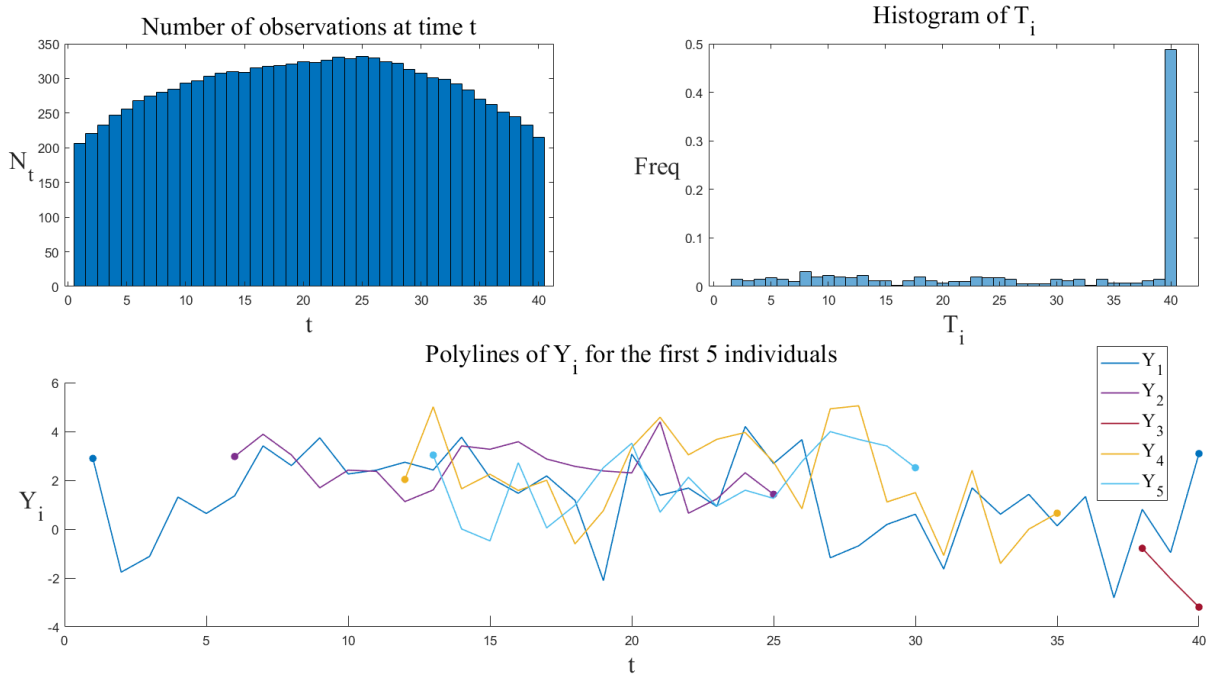


Figure 2: Characteristics of the unbalanced panel we generated

Figure 2 illustrates key features of the simulated unbalanced dynamic network panel data with $N = 400$, $T = 40$ and $UP = 31.7\%$. It reveals that the number of observed nodes peaks during intermediate stages, with sparser observations in initial and terminal phases. About 30% of nodes

are fully observed over the entire $T + 1$ periods, while the remaining nodes display uniformly distributed observation durations.

4.2 Simulation Results

In our simulation study, we investigate the performance of both the QMLE estimator and its bias-corrected counterpart under varying configurations of $N \in \{100, 400, 1600\}$, $T \in \{10, 40\}$, and $UP \in \{30\%, 60\%\}$. We simulate data under two true parameter settings: $\theta_0 = (0.5, 0.2, 0.1, 1, 1, 1)$ or $\theta_0 = (0.1, 0.3, 0.5, 1, 1, 1)$, where $\theta_0 = (\rho_0, \lambda_0, \nu_0, \gamma_0, \beta_0, \sigma_0^2)$. Additionally, we consider three error distributions: normal, centered exponential, and Laplace. Under each setting, the estimation is repeated 1,000 times, then we evaluate the bias, standard deviation (SD), root mean square error (RMSE), and coverage probability (CP) of the estimators.

The simulation results are presented in Tables 1-2 and Tables D.1-D.6 in Supplementary Appendix D.1. From the tables, we obtain the following findings.

- (1) The biases of both the original estimator and the bias-corrected estimator decrease significantly as T increases, but show little change as N increases. Moreover, for fixed N and T , a higher UP leads to larger bias. These findings are broadly consistent with the theoretical bias of order $O_p(\frac{1}{c_u T})$.
- (2) Regardless of whether bias correction is applied, the standard deviations of most estimators are approximately halved when either N or T is quadrupled, consistent with the theoretical convergence rate of $1/\sqrt{n}$. An exception is $\hat{\gamma}$, whose standard deviation remains essentially unchanged as T increases, aligning with the theoretical convergence rate of $1/\sqrt{c_u N}$. Moreover, the standard deviation increases as the UP rises.
- (3) The original estimators exhibit substantial bias, especially for ν and σ^2 , while the bias-corrected estimators significantly reduce the bias. The bias-corrected estimators show notable

improvements in both bias and RMSE, and their CPs are also closer to the nominal levels of 95% and 90%.

(4) As N increases, there is a downward trend in CPs for both estimators, which is attributable to the asymptotic bias of order $O_p(\sqrt{N/T^3})$.

To examine the correctness of the asymptotic theory, we plot the kernel density curves of $\frac{\hat{\theta}_i - \theta_{0i}}{\text{SE}_i}$, and $\frac{\hat{\theta}_i^1 - \theta_{0i}}{\text{SE}_i}$, where $\hat{\theta}_i$, $\hat{\theta}_i^1$ and θ_{0i} denote the i -th element of $\hat{\theta}$, $\hat{\theta}^1$ and θ_0 , respectively, and SE_i denotes the square root of the i -th diagonal element of $\Sigma_{\theta_0, n}^{-1} (\Sigma_{\theta_0, n} + \Omega_{\theta_0, n}) \Sigma_{\theta_0, n}^{-1}$. These kernel densities are then compared with the probability density function (PDF) of the standard normal distribution. The results are shown in Figures 3, 4 and D.1-D.6 in Supplementary Appendix D.2. As illustrated in the figures, regardless of whether the estimators are bias corrected or not, their distributions become increasingly close to normality as the sample size increases. The bias-corrected estimators exhibit distributions that are closer to a centered normal distribution than the original ones.

Table 1: Results of estimator with Normal error, UP=30%, $\theta_0 = (0.5, 0.2, 0.1, 1, 1, 1)$.

		ρ	λ	ν	γ	β	σ^2			ρ	λ	ν	γ	β	σ^2		
$T = 10$								$T = 40$									
$N = 100$	BIAS	-0.0044	0.0327	-0.0753	-0.0348	-0.0098	-0.1594	$N = 100$	BIAS	0.0006	0.0077	-0.0191	-0.0014	-0.0016	-0.0399		
	SD	0.0268	0.0367	0.0299	0.1497	0.0427	0.0511		SD	0.0124	0.0178	0.0146	0.1426	0.0191	0.0275		
	RMSE	0.0271	0.0492	0.0810	0.1537	0.0438	0.1674		RMSE	0.0124	0.0194	0.0240	0.1426	0.0192	0.0484		
	95%CP	0.9340	0.8620	0.2810	0.9470	0.9370	0.1530		95%CP	0.9550	0.9190	0.7070	0.9510	0.9570	0.6860		
	90%CP	0.8640	0.7660	0.1920	0.8900	0.8890	0.0930		90%CP	0.8910	0.8740	0.6080	0.8970	0.9060	0.5630		
		Before bias correction								Before bias correction							
		BIAS	-0.0034	0.0061	-0.0159	-0.0064	-0.0005	-0.0397			BIAS	0.0002	0.0001	-0.0010	0.0019	-0.0007	-0.0053
		SD	0.0267	0.0375	0.0311	0.1495	0.0426	0.0580			SD	0.0124	0.0180	0.0148	0.1425	0.0191	0.0284
		RMSE	0.0269	0.0380	0.0349	0.1497	0.0426	0.0703			RMSE	0.0124	0.0180	0.0149	0.1425	0.0191	0.0289
		95%CP	0.9360	0.9380	0.9100	0.9470	0.9410	0.8770			95%CP	0.9550	0.9490	0.9430	0.9530	0.9560	0.9420
		90%CP	0.8670	0.9000	0.8380	0.8990	0.8920	0.7780			90%CP	0.8890	0.8950	0.8820	0.8960	0.9020	0.8900
$T = 10$								$T = 40$									
$N = 400$	BIAS	-0.0021	0.0339	-0.0748	-0.0341	-0.0126	-0.1525	$N = 400$	BIAS	0.0000	0.0082	-0.0194	-0.0027	0.0001	-0.0364		
	SD	0.0136	0.0189	0.0146	0.0765	0.0207	0.0259		SD	0.0063	0.0090	0.0070	0.0705	0.0098	0.0142		
	RMSE	0.0137	0.0388	0.0762	0.0838	0.0242	0.1546		RMSE	0.0063	0.0122	0.0206	0.0706	0.0098	0.0391		
	95%CP	0.9360	0.5630	0.0010	0.9080	0.9070	0.0000		95%CP	0.9540	0.8640	0.2120	0.9590	0.9500	0.2440		
	90%CP	0.8730	0.4490	0.0000	0.8450	0.8370	0.0000		90%CP	0.9080	0.7630	0.1390	0.9020	0.8930	0.1700		
		Before bias correction								Before bias correction							
		BIAS	-0.0012	0.0064	-0.0152	-0.0065	-0.0033	-0.0319			BIAS	-0.0004	0.0006	-0.0013	0.0004	0.0010	-0.0017
		SD	0.0136	0.0194	0.0151	0.0768	0.0206	0.0294			SD	0.0063	0.0091	0.0071	0.0707	0.0098	0.0146
		RMSE	0.0136	0.0204	0.0214	0.0771	0.0208	0.0434			RMSE	0.0063	0.0091	0.0072	0.0707	0.0099	0.0147
		95%CP	0.9330	0.9350	0.8290	0.9260	0.9540	0.7590			95%CP	0.9500	0.9460	0.9420	0.9590	0.9450	0.9310
		90%CP	0.8750	0.8670	0.7260	0.8730	0.9000	0.6690			90%CP	0.9020	0.9040	0.8830	0.9010	0.9010	0.8670
$T = 10$								$T = 40$									
$N = 1600$	BIAS	-0.0020	0.0338	-0.0748	-0.0343	-0.0114	-0.1530	$N = 1600$	BIAS	0.0004	0.0078	-0.0192	-0.0033	-0.0011	-0.0371		
	SD	0.0071	0.0090	0.0075	0.0357	0.0102	0.0127		SD	0.0032	0.0047	0.0034	0.0352	0.0048	0.0067		
	RMSE	0.0073	0.0350	0.0751	0.0496	0.0153	0.1535		RMSE	0.0032	0.0090	0.0195	0.0354	0.0049	0.0377		
	95%CP	0.9300	0.0480	0.0000	0.8550	0.8100	0.0000		95%CP	0.9530	0.6140	0.0010	0.9500	0.9520	0.0010		
	90%CP	0.8630	0.0210	0.0000	0.7690	0.6980	0.0000		90%CP	0.9020	0.4960	0.0010	0.8970	0.8920	0.0000		
		Before bias correction								Before bias correction							
		BIAS	-0.0011	0.0062	-0.0152	-0.0067	-0.0022	-0.0325			BIAS	0.0000	0.0002	-0.0011	-0.0001	-0.0002	-0.0025
		SD	0.0071	0.0094	0.0078	0.0359	0.0102	0.0144			SD	0.0032	0.0047	0.0034	0.0352	0.0048	0.0069
		RMSE	0.0072	0.0112	0.0171	0.0365	0.0104	0.0355			RMSE	0.0032	0.0047	0.0036	0.0352	0.0048	0.0073
		95%CP	0.9310	0.9000	0.4840	0.9530	0.9450	0.3380			95%CP	0.9580	0.9450	0.9450	0.9490	0.9580	0.9360
		90%CP	0.8720	0.8330	0.3690	0.9040	0.9060	0.2280			90%CP	0.9000	0.8900	0.8830	0.8960	0.9070	0.8790

Notes: $UP = 1 - \frac{n}{NT}$. In the table, **bold** numbers indicate that the bias-corrected results have improved, while *italicized* numbers indicate that the bias-corrected results perform equally well as before. The 95%CP and 90%CP indicate the frequencies that the true parameter value is contained within the 95% and 90% confidence intervals of the estimator, respectively.

Table 2: Results of estimator with Normal error, UP=60%, $\theta_0 = (0.5, 0.2, 0.1, 1, 1, 1)$.

		ρ	λ	ν	γ	β	σ^2			ρ	λ	ν	γ	β	σ^2
$T = 10$								$T = 40$							
$N = 100$	BIAS	-0.0093	0.0605	-0.1358	-0.0929	-0.0337	-0.2862	$N = 100$	BIAS	0.0004	0.0141	-0.0321	-0.0147	-0.0029	-0.0694
	SD	0.0307	0.0468	0.0440	0.1348	0.0613	0.0613		SD	0.0141	0.0203	0.0185	0.1098	0.0263	0.0352
	RMSE	0.0321	0.0765	0.1428	0.1638	0.0700	0.2927		RMSE	0.0141	0.0247	0.0370	0.1108	0.0264	0.0778
	95%CP	0.9100	0.7650	0.1200	0.8810	0.9000	0.0100		95%CP	0.9470	0.9070	0.6060	0.9570	0.9410	0.5100
	90%CP	0.8370	0.6700	0.0670	0.8260	0.8310	0.0020		90%CP	0.8870	0.8320	0.4840	0.9040	0.8990	0.3840
		Before bias correction								Before bias correction					
	BIAS	-0.0062	0.0212	-0.0481	-0.0345	-0.0112	-0.1083		BIAS	0.0000	0.0000	-0.0031	-0.0074	-0.0006	-0.0105
	SD	0.0308	0.0484	0.0458	0.1341	0.0612	0.0744		SD	0.0141	0.0206	0.0188	0.1099	0.0262	0.0371
	RMSE	0.0314	0.0528	0.0664	0.1385	0.0623	0.1314		RMSE	0.0141	0.0206	0.0191	0.1102	0.0262	0.0386
	95%CP	0.9200	0.9180	0.7850	0.9380	0.9430	0.6750		95%CP	0.9460	0.9490	0.9500	0.9590	0.9460	0.9310
	90%CP	0.8490	0.8530	0.6910	0.8710	0.8740	0.5500		90%CP	0.8880	0.9170	0.8890	0.9090	0.9030	0.8840
$T = 10$								$T = 40$							
$N = 400$	BIAS	-0.0061	0.0583	-0.1302	-0.0861	-0.0316	-0.2766	$N = 400$	BIAS	0.0003	0.0145	-0.0317	-0.0069	-0.0026	-0.0660
	SD	0.0153	0.0225	0.0215	0.0645	0.0300	0.0311		SD	0.0068	0.0101	0.0094	0.0573	0.0129	0.0177
	RMSE	0.0165	0.0625	0.1320	0.1076	0.0435	0.2784		RMSE	0.0068	0.0176	0.0331	0.0577	0.0131	0.0683
	95%CP	0.9050	0.2960	0.0000	0.7510	0.8230	0.0000		95%CP	0.9470	0.7290	0.0810	0.9430	0.9450	0.0410
	90%CP	0.8260	0.1980	0.0000	0.6390	0.7240	0.0000		90%CP	0.8990	0.6200	0.0390	0.8840	0.9120	0.0220
		Before bias correction								Before bias correction					
	BIAS	-0.0032	0.0179	-0.0426	-0.0282	-0.0095	-0.0963		BIAS	-0.0001	0.0009	-0.0028	0.0004	-0.0003	-0.0071
	SD	0.0152	0.0232	0.0221	0.0635	0.0299	0.0378		SD	0.0068	0.0103	0.0096	0.0570	0.0129	0.0187
	RMSE	0.0156	0.0293	0.0479	0.0695	0.0313	0.1035		RMSE	0.0068	0.0103	0.0100	0.0570	0.0129	0.0200
	95%CP	0.9230	0.8910	0.4940	0.9320	0.9360	0.2560		95%CP	0.9470	0.9470	0.9320	0.9390	0.9510	0.9250
	90%CP	0.8560	0.8090	0.3820	0.8830	0.8850	0.1660		90%CP	0.8940	0.9000	0.8740	0.8980	0.9110	0.8710
$T = 10$								$T = 40$							
$N = 1600$	BIAS	-0.0055	0.0591	-0.1305	-0.0868	-0.0329	-0.2748	$N = 1600$	BIAS	0.0003	0.0147	-0.0319	-0.0083	-0.0025	-0.0653
	SD	0.0077	0.0118	0.0108	0.0322	0.0152	0.0155		SD	0.0035	0.0050	0.0047	0.0268	0.0066	0.0091
	RMSE	0.0095	0.0602	0.1310	0.0926	0.0363	0.2752		RMSE	0.0035	0.0155	0.0323	0.0281	0.0070	0.0659
	95%CP	0.8560	0.0020	0.0000	0.2400	0.4000	0.0000		95%CP	0.9500	0.1890	0.0000	0.9500	0.9380	0.0000
	90%CP	0.7740	0.0010	0.0000	0.1650	0.2880	0.0000		90%CP	0.8980	0.1120	0.0000	0.8970	0.8770	0.0000
		Before bias correction								Before bias correction					
	BIAS	-0.0028	0.0185	-0.0427	-0.0287	-0.0109	-0.0940		BIAS	-0.0002	0.0011	-0.0031	-0.0010	-0.0003	-0.0064
	SD	0.0076	0.0122	0.0114	0.0320	0.0151	0.0187		SD	0.0035	0.0051	0.0048	0.0269	0.0066	0.0096
	RMSE	0.0081	0.0222	0.0442	0.0430	0.0186	0.0959		RMSE	0.0035	0.0052	0.0057	0.0269	0.0066	0.0115
	95%CP	0.9020	0.6440	0.0230	0.8600	0.8880	0.0000		95%CP	0.9480	0.9540	0.8960	0.9710	0.9520	0.8850
	90%CP	0.8490	0.5270	0.0100	0.7800	0.7980	0.0000		90%CP	0.8970	0.9090	0.8180	0.9070	0.9080	0.7870

Notes: $UP = 1 - \frac{n}{NT}$. In the table, **bold** numbers indicate that the bias-corrected results have improved, while *italicized* numbers indicate that the bias-corrected results perform equally well as before. The 95%CP and 90%CP indicate the frequencies that the true parameter value is contained within the 95% and 90% confidence intervals of the estimator, respectively.

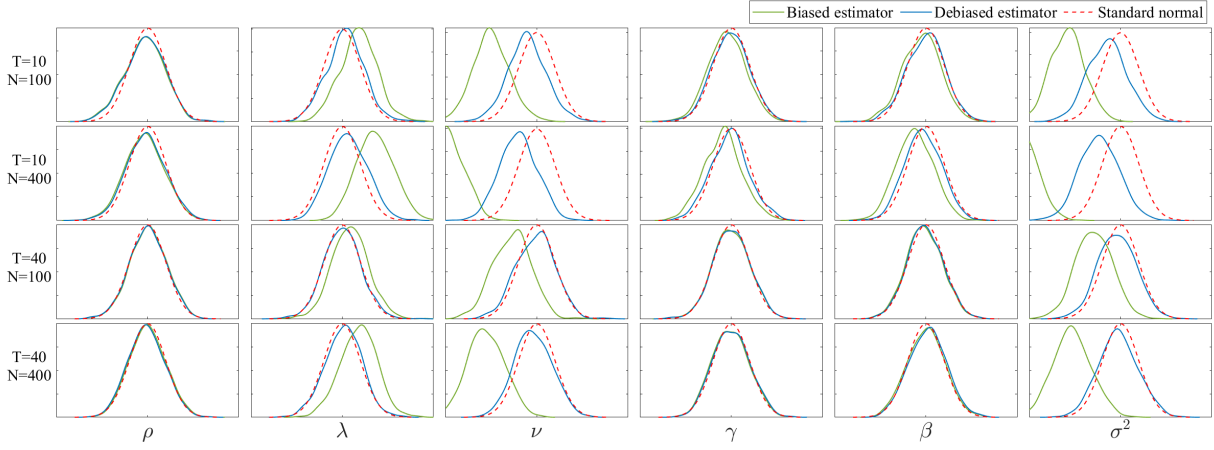


Figure 3: PDF of standardized estimator with normal error, UP=30%, $\theta_0 = (0.5, 0.2, 0.1, 1, 1, 1)$

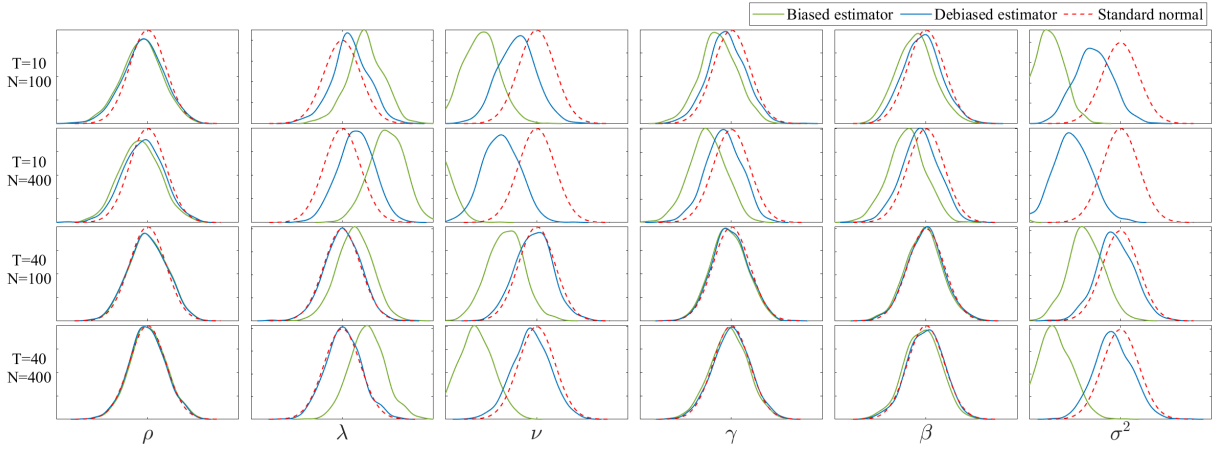


Figure 4: PDF of standardized estimator with normal error, UP=60%, $\theta_0 = (0.5, 0.2, 0.1, 1, 1, 1)$

5 Real Data Analysis

To assess our model's ability to capture the dynamics of unbalanced spatio-temporal panel data, we take the short-term rental market as the empirical application. In recent years, Airbnb, as a leading global platform for short-term accommodation, has expanded rapidly across cities and regions, and its supply and pricing dynamics have attracted extensive academic attention. More importantly, Airbnb data naturally exhibit an unbalanced panel structure: the set of available listings is not identical across time periods, and many listings are only intermittently observed. This provides a representative and complex empirical setting for our study. A large body of literature has already

examined the rental pricing of Airbnb properties, such as the studies by [Zhang et al. \(2017\)](#), [Gyódi & Łukasz Nawaro \(2021\)](#), and [Wang & Song \(2023\)](#), which apply spatial econometric methods to cross-sectional data of Airbnb listings. [Jiménez et al. \(2022\)](#) employs an unbalanced dynamic panel data model to analyze the impact of Airbnb listings on the Spanish tourism markets. Their model does not account for the spatial dependence in the data. [Gunter et al. \(2020\)](#) uses a static spatial panel model to explore the substitution or complementarity relationship between Airbnb and traditional accommodations. However, their analysis is restricted to a balanced subsample of listings that are continuously observed over a long period, which accounts for less than 10% of the total sample. This balanced spatial panel model neglects the spatial spillover effects from short-lived listings and does not account for the temporal dynamics in rental prices. While there have been studies using various models to analyze Airbnb rental prices, none simultaneously account for spatial spillover effects, temporal dynamics (e.g., price lags), and the unbalanced nature of the panel data. This is precisely what our model is designed to achieve.

We collect listing data from Airbnb for two regions: New Zealand and New York City³. The New Zealand dataset contains 30 monthly periods from May 2023 to October 2025, with approximately 50,000 listings per period. The New York City dataset contains 17 monthly periods from June 2024 to October 2025, with approximately 20,000 listings per period. Each listing includes information such as rental price, geographic coordinates, availability of the listing over the next 30 days, and the number of reviews in the past 30 days, among others. To examine how the dynamics of the short-term rental market vary across areas and at different spatial scales, we select six areas for our analysis: Auckland, Queenstown-Lakes District, and Christchurch City in New Zealand, and Williamsburg, Midtown, and Hell's Kitchen in New York City. Within each area, to study the dynamic determinants of rental prices, we use the logarithm of rental price as the dependent variable.

³<https://insideairbnb.com>

The unbalanced panel for Auckland is visualized in Figure 5, which consists of 16,315 units observed over 30 periods. The figure shows that the number of observations in each period is close to 8,000 and the overall degree of unbalancedness of the panel is $UP = 48.65\%$. In addition, the degree of unbalancedness is 41.90% for Queenstown, 46.86% for Christchurch, 33.86% for Williamsburg, 32.43% for Midtown, and 36.15% for Hell's Kitchen. The descriptive statistics of each data set are detailed in Supplementary Appendix E, Table E.1.

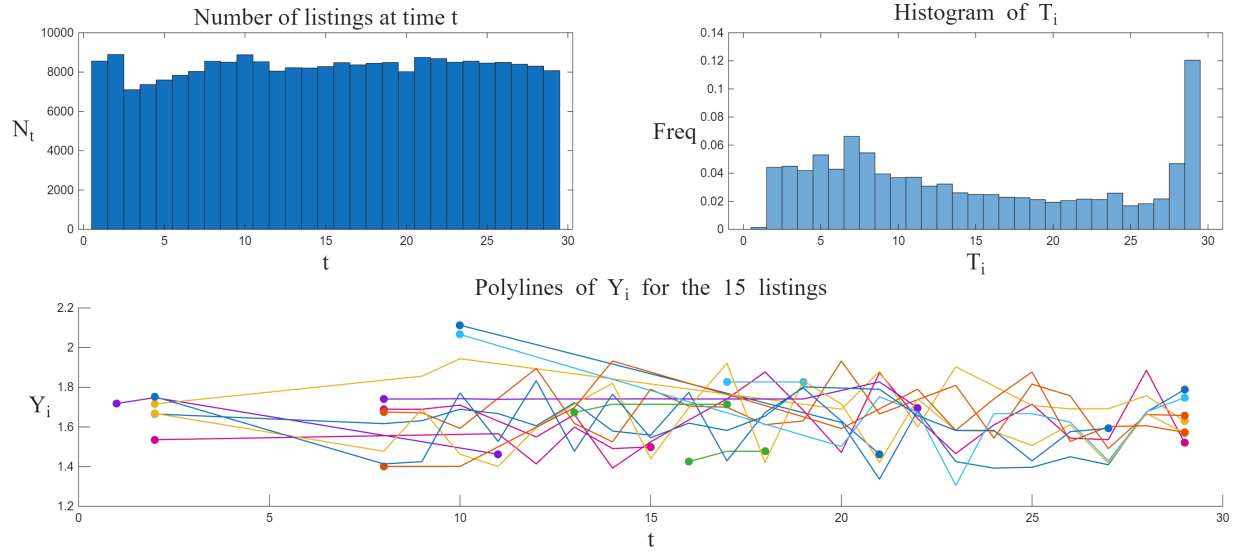


Figure 5: Characteristics of the unbalanced panel of the listing data in Auckland

Figures 6 and 7 display the geographical distribution of log rental prices for listings in Midtown and Queenstown, respectively. The color shading corresponds to the magnitude of log rental price, with darker tones indicating lower values. These figures show that the log rental prices exhibit obvious spatial and temporal correlation. Based on the data described above, we construct the unbalanced dynamic network panel model as in equation (2). We include a listing-specific covariate measuring the number of available days in the next 30 days (avail30d) and a neighborhood-level covariate defined as the average number of available days in the next 30 days among listings within 1 km (avgAvail30d1km). Furthermore, a binary covariate indicating whether the listing is in the local peak tourism season is introduced to mitigate the impact of temporal heterogeneity⁴. We

⁴The designation of peak tourism seasons is based on official visitor arrival statistics from Tourism New Zealand

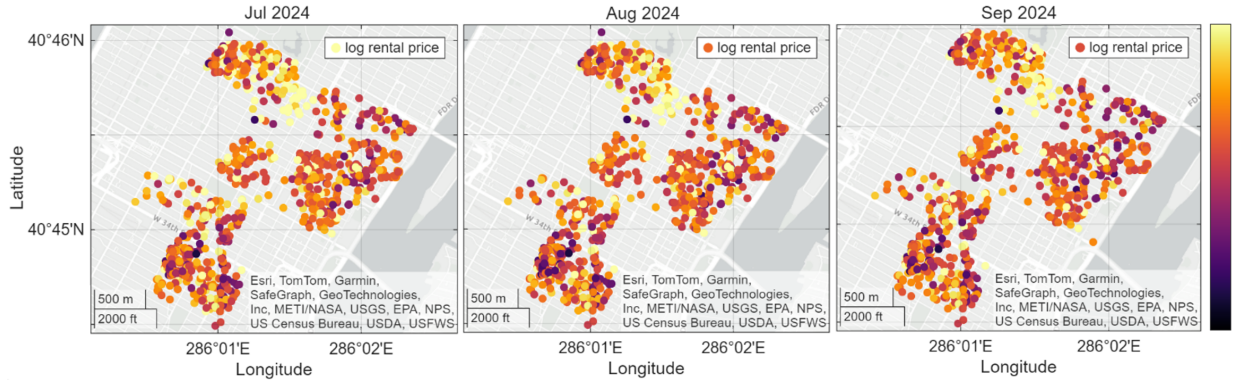


Figure 6: Geographical distribution of log rental prices in Midtown

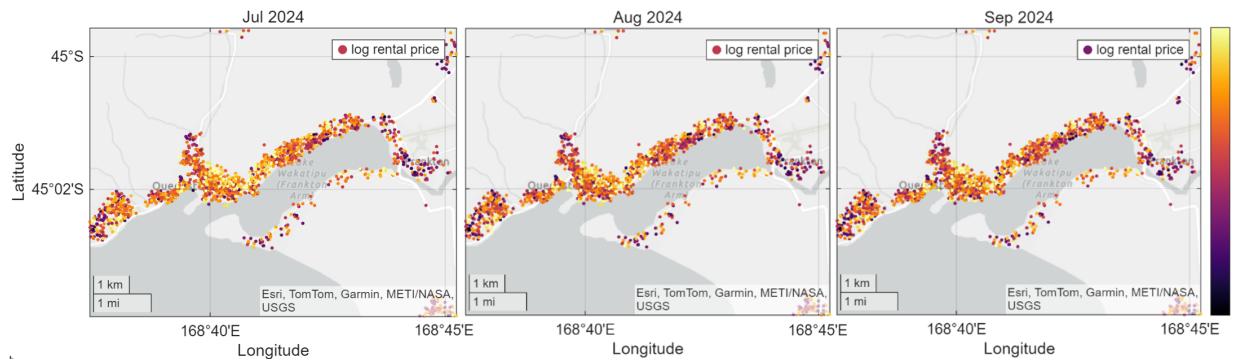


Figure 7: Geographical distribution of log rental prices in Queenstown

consider constructing the network adjacency matrix as a binary distance-band matrix, in which two nodes are connected if the geographical distance between them does not exceed d kilometers. We consider three alternative values of d , namely $d = 0.5, 1$ and 2 , to check the robustness. Based on this specification, we define W_t as the row-normalized adjacency matrix in period t , and M_t as a row-normalized binary distance-band matrix constructed between units observed in periods t and $t - 1$, which captures network spillovers originating in the previous period.

Tables 3 and 4 compare the estimation results across areas under the same model specification. The estimation results are similar across areas within New Zealand and within New York City, but differ markedly between the two settings. We obtain the following findings based on the estimated results:

(<https://www.tourismnewzealand.com/>), which show that international tourist inflows peak between December and February. For New York City, although there is no official definition of peak tourism months, May, September, and December are classified as peak seasons based on widely accepted conventions in the tourism and hospitality literature.

- (1) The network autoregressive coefficient captures contemporaneous interaction effects among connected listings. We find that this coefficient is not only uniformly positive across all six areas but also dramatically larger in New York City than in New Zealand: estimates range from 0.64 to 0.83 in NYC neighborhoods, compared to just 0.09 to 0.24 in New Zealand regions. This difference likely reflects the higher listing density and greater market liquidity in New York City, which facilitate rapid transmission of price information and intensify real-time competitive pressure. In contrast, listings in New Zealand are more geographically dispersed, resulting in weaker contemporaneous spatial transmission.
- (2) The lagged network autoregressive effect captures the impact of neighboring prices in the previous period on current rental prices. This effect is significantly negative across all areas, indicating that higher past prices among connected neighbors are associated with lower current prices. Moreover, regions exhibiting stronger contemporaneous network interactions tend to have more negative lagged network coefficients. This pattern suggests an intertemporal dampening mechanism in network spillovers, whereby contemporaneous spatial interactions are partially attenuated by subsequent network effects.
- (3) The temporal lagged effect is estimated to be significantly positive across all areas, indicating the presence of rental price stickiness.
- (4) The coefficients on avail30d and avgAvail30d1km capture how a listing's price responds to its own supply scarcity and that of its local competitors. Most coefficients are significantly negative. That means, if there are more available days for this listing or listings nearby in the following days, the price will tend to decrease, which is consistent with economic intuition.
- (5) The estimates for the peak season are all positive, which is in line with the fact that hosts tend to raise prices during high-demand periods.

Furthermore, Tables E.2–E.7 in Supplementary Appendix E report detailed estimation results

Table 3: Estimation results across areas in New Zealand with network adjacency matrix (2km)

	Auckland	Queenstown	Christchurch
ρ ($W_t Y_t$)	0.0879(0.0023)***	0.2404(0.0046)***	0.1010(0.0054)***
λ ($M_t Y_{t-1}$)	-0.0678(0.0019)***	-0.1478(0.0028)***	-0.0783(0.0042)***
ν (Y_{t-1})	0.2860(0.0015)***	0.3151(0.0022)***	0.4040(0.0030)***
avail30d	-0.0004(0.0001)***	-0.0010(0.0001)***	-0.0005(0.0001)***
avgAvail30d1km	-0.0054(0.0001)***	-0.0090(0.0002)***	-0.0055(0.0003)***
Peak season	0.0142(0.0011)***	0.0173(0.0015)***	0.0330(0.0021)***
Listing effect	0.2111(0.0020)***	0.1871(0.0031)***	0.3039(0.0041)***
<i>N</i>	16315	8380	4829
<i>T</i>	29	29	29
<i>n</i>	240585	141188	74411
UP	49.15%	41.90%	46.86%

Notes: Estimates are presented with their standard errors in parentheses. Statistical significance is indicated by stars: *** for $p < 0.01$, ** for $p < 0.05$, and * for $p < 0.1$.

Table 4: Estimation results across areas in New York City with network adjacency matrix (2km)

	Williamsburg	Midtown	Hell's Kitchen
ρ ($W_t Y_t$)	0.7452(0.0594)***	0.8269(0.0359)***	0.6382(0.0361)***
λ ($M_t Y_{t-1}$)	-0.3777(0.0499)***	-0.3696(0.0200)***	-0.2569(0.0125)***
ν (Y_{t-1})	0.4183(0.0069)***	0.4431(0.0073)***	0.4186(0.0069)***
avail30d	0.0009(0.0003)***	-0.0014(0.0004)***	-0.0004(0.0003)
avgAvail30d1km	-0.0132(0.0036)***	-0.0074(0.0050)	-0.0156(0.0030)***
Peak season	0.0128(0.0051)**	0.0063(0.0064)	0.0186(0.0058)***
Listing effect	0.0539(0.0626)	0.1173(0.0277)***	0.2154(0.0157)***
<i>N</i>	1218	1990	1460
<i>T</i>	16	16	16
<i>n</i>	12890	21515	14916
UP	33.86%	32.43%	36.15%

Notes: Estimates are presented with their standard errors in parentheses. Statistical significance is indicated by stars: *** for $p < 0.01$, ** for $p < 0.05$, and * for $p < 0.1$.

under different network weight matrix specifications for each area. Within each area, the estimation results are generally similar across different specifications. An exception arises for the network autoregressive coefficient and the lagged network autoregressive effect in the New Zealand areas, whose absolute magnitudes increase as the distance threshold d in the spatial weight matrix expands. This pattern likely reflects the more geographically dispersed distribution of listings in New Zealand, such that larger neighborhood definitions capture additional relevant spatial interactions.

6 Conclusion

In this paper, we consider the QMLE for a genuinely unbalanced dynamic network panel data model with individual fixed effects as both N and T go to infinity. The QMLE is \sqrt{NT} -consistent for all parameters, except for the listing effect $\hat{\gamma}$, which achieves \sqrt{N} -consistency. While the QMLE is asymptotically biased when N grows asymptotically faster than T , the bias-corrected estimator we propose is asymptotically unbiased and normally distributed as long as $\frac{N}{T^3} \rightarrow 0$.

There are several extensions of this paper: (1) We are studying the GMM estimation for this model, as GMM allows for heteroskedasticity in the error terms, and is still consistent when T is finite. (2) Building on this framework, temporal heterogeneous effects can also be incorporated into the model. In particular, extending the model to allow for two-way fixed effects and individual-time interactive fixed effects constitutes an important direction for future research. (3) A more complex mechanism for the listing effect is another promising extension.

Supplementary Material

The supplementary material includes the required lemmas and their proofs, the explicit expressions and properties of the QMLE score function and Hessian matrix, detailed proofs of the theorems, as well as tables and figures for the simulation and empirical results.

Acknowledgments

This work is supported by the National Natural Science Foundation of China (NNSFC) (72473118, 72333001, 71988101). We also thank Professor Xiaoyu Meng, Chao Yang, Fei Jin, and Kai Yang for their valuable comments.

Declaration of Generative AI and AI-assisted Technologies in the Writing Process

During the preparation of this work the authors used ChatGPT in order to enhance the writing quality. After using this tool/service, the authors reviewed and edited the content as needed and take full responsibility for the content of the publication.

References

Amidi, S., Fagheh Majidi, A. & Javaheri, B. (2020), 'Growth spillover: a spatial dynamic panel data and spatial cross section data approaches in selected asian countries', *Future Business Journal* **6**(1), 20.

Billé, A. G. & Caporin, M. (2022), 'Impact of COVID-19 on financial returns: a spatial dynamic panel data model with random effects', *Journal of Spatial Econometrics* **3**(1), 1–21.

Chang, H.-Y., Wang, W. & Yu, J. (2021), 'Revisiting the environmental kuznets curve in china: A spatial dynamic panel data approach', *Energy Economics* **104**, 105600.

Gunter, U., Önder, I. & Zekan, B. (2020), 'Modeling airbnb demand to new york city while employing spatial panel data at the listing level', *Tourism Management* **77**, 104000.

Gyódi, K. & Łukasz Nawaro (2021), 'Determinants of airbnb prices in european cities: A spatial econometrics approach', *Tourism Management* **86**, 104319.

Han, X., Hsieh, C.-S. & Ko, S. I. M. (2021), 'Spatial modeling approach for dynamic network formation and interactions', *Journal of Business & Economic Statistics* **39**(1), 120–135.

Honoré, B. E. (1992), 'Trimmed lad and least squares estimation of truncated and censored regression models with fixed effects', *Econometrica* **60**(3), 533–565.

Honoré, B. E. & Hu, L. (2004), ‘Estimation of cross sectional and panel data censored regression

models with endogeneity’, *Journal of Econometrics* **122**(2), 293–316.

Hu, L. (2002), ‘Estimation of a censored dynamic panel data model’, *Econometrica* **70**(6), 2499–2517.

Jenish, N. & Prucha, I. R. (2012), ‘On spatial processes and asymptotic inference under near-epoch dependence’, *Journal of Econometrics* **170**(1), 178–190.

Jiménez, J. L., Ortúñoz, A. & Pérez-Rodríguez, J. V. (2022), ‘How does airbnb affect local spanish tourism markets?’, *Empirical Economics* **62**(5), 2515–2545.

Kapoor, M., Kelejian, H. H. & Prucha, I. R. (2007), ‘Panel data models with spatially correlated error components’, *Journal of Econometrics* **140**(1), 97–130.

Kyriazidou, E. (1997), ‘Estimation of a panel data sample selection model’, *Econometrica* **65**(6), 1335–1364.

Lee, L. F. (2004), ‘Asymptotic distributions of quasi-maximum likelihood estimators for spatial autoregressive models’, *Econometrica* **72**(6), 1899–1925.

Lee, L. F. (2007), ‘GMM and 2SLS estimation of mixed regressive, spatial autoregressive models’, *Journal of Econometrics* **137**(2), 489–514.

Lee, L. F. & Yu, J. (2010), ‘A spatial dynamic panel data model with both time and individual fixed effects’, *Econometric Theory* **26**(2), 564–597.

Lee, L. F. & Yu, J. (2012), ‘QML estimation of spatial dynamic panel data models with time varying spatial weights matrices’, *Spatial Economic Analysis* **7**(1), 31–74.

Lee, L. F. & Yu, J. (2014), ‘Efficient GMM estimation of spatial dynamic panel data models with fixed effects’, *Journal of Econometrics* **180**(2), 174–197.

Meng, X. & Yang, Z. (2025a), ‘Fixed effects estimation of spatial panel model with missing

responses: An application to us state tax competition', *Journal of Business & Economic Statistics*. In press.

Meng, X. & Yang, Z. (2025b), 'Genuinely unbalanced spatial panel data models: fixed effects m-estimation and inference', *Econometric Review*. In press.

Qu, X., Lee, L. F. & Yu, J. (2017), 'QML estimation of spatial dynamic panel data models with endogenous time varying spatial weights matrices', *Journal of Econometrics* **197**(2), 173–201.

Sasaki, Y. & Xin, Y. (2017), 'Unequal spacing in dynamic panel data: Identification and estimation', *Journal of Econometrics* **196**(2), 320–330.

Su, L., Wang, F. & Wang, Y. (2025), 'Estimation and Inference for Unbalanced Panel Data Models with Interactive Fixed Effects'. Working paper, SSRN. DOI: 10.2139/ssrn.5177283.

Wang, Z. & Song, Y. (2023), 'Deep learning for the spatial additive autoregressive model with nonparametric endogenous effect', *Spatial Statistics* **55**, 100743.

Wooldridge, J. M. (1995), 'Selection corrections for panel data models under conditional mean independence assumptions', *Journal of Econometrics* **68**(1), 115–132.

Wu, Z., Jiang, W. & Xu, X. (2025), 'Applications of functional dependence to spatial econometrics', *Econometric Theory* **41**(5), 1044–1079.

Yu, J., de Jong, R. & Lee, L. F. (2008), 'Quasi-maximum likelihood estimators for spatial dynamic panel data with fixed effects when both n and T are large', *Journal of Econometrics* **146**(1), 118–134.

Zhang, Z., Chen, R. J. C., Han, L. D. & Yang, L. (2017), 'Key factors affecting the price of airbnb listings: A geographically weighted approach', *Sustainability* **9**(9).